JAASCI
http://jaasci.com
JOURNAL OF ADVANCED APPLIED SCIENCES
e-ISSN: 2979-9759
PRENSIP
https://prensip.gen.tr

RESEARCH ARTICLE

# Deuteron Optical Model Calculations for Elastic and Inelastic Reactions on $^{14}N$, $^{16}O$, $^{27}Al$ Target Nuclei

Halim Büyükuslu

Giresun University, Espiye Vocational School, Giresun/Türkiye

**ARTICLE INFO**

**Article History**
Received: 08.11.2023
Accepted: 27.11.2023
First Published: 18.12.2023

**Keywords**
Angular distribution
Elastic and inelastic scattering
Optical model
Talys

**ABSTRACT**

Nuclear reaction cross sections have a key role in nuclear radioisotope production research. It is also an important part of applied fields such as energy production and experimental nuclear studies. It has been the subject of theoretical studies such as elucidating the nuclear structure and preparing and testing nuclear reaction models. It has become a very useful tool, especially for determining nuclear optical model parameters. In this study differential cross sections were calculated for elastic and inelastic scattering of 14-15 MeV energy range deuterons from $^{14}N$, $^{16}O$ and $^{27}Al$. Calculation were carried out with TALYS 1.96/2.0 nuclear reaction code. Calculations include determining the deuteron optical model that match the experimental data. The values calculated with theoretical models were compared with experimental data obtained from the literature. While such studies are important for testing nuclear reaction models, they are also important for encouraging the preparation of nuclear reaction codes.

**Please cite this paper as follows:**

Büyükuslu, H. (2023). Deuteron optical model calculations for elastic and inelastic reactions on $^{14}N$, $^{16}O$, $^{27}Al$ target nuclei. *Journal of Advanced Applied Sciences*, *2*(2), 68-72. https://doi.org/10.61326/jaasci.v2i2.112

## 1. Introduction

Phenomenological nuclear optical model (NOM) contributes greatly to the understanding of nuclear structure through the valuable data it provides. NOM, in which the interaction of the incoming particle and the target nucleus is represented by a complex potential, also provides useful data to other nuclear models such as total reaction cross section, transmission coefficient, potential scattering radius etc. In the model, the total potential is defined through parameters and potential depths. In order to increase the precision of the calculation results in the optical model, it is very important to choose the correct model parameters and potential depths. The number, diversity and currentness of experimental data on elastic and inelastic scattering reactions increase the success of the nuclear optical model. The number of experimental studies on nuclear scattering reactions included deuteron is relatively low compared to the experimental studies on the scattering reactions of neutron and proton-inducted reactions. This situation causes theoretical deuteron optical model studies to remain relatively limited.

Comparing nuclear models is a useful process to test the success of the models. In this way, the incident energy values and the target nucleus mass ranges where the models are successful (or not) can be determined (Büyükuslu, 2017). Nuclear reaction codes have become the most important tools of theoretical calculations. Comparison studies of reaction

Correspondence
E-mail address: halimbuyukuslu@gmail.com

models also contribute to the development of nuclear reaction codes and increasing the variety of models they contain.

In this study, differential cross sections of elastic and inelastic scattering reactions involving deuteron projectile particles were obtained for $^{14}N$, $^{16}O$ and $^{27}Al$ target nuclei. Calculations were carried out for five different deuteron optical potentials. Obtained results were compared with experimental data. The common use and general expression of the nuclear optical model are given in the next section. References are given to access detailed explanations of the nuclear optical models mentioned in the article.

## 2. Theoretical Model

Phenomenological nuclear optical model potential, which includes the terms volume, surface and spin-orbit, is expressed as follows:

$$U_{opt}(r) = +\vartheta_c(r) \quad -Vf_V(r) + V_S g_V(r) - iW_S g_W(r) - iW_V f_W(r) - d_{SO}\vec{l}\cdot\vec{s}V_{SO}h_{V_{SO}}(r) + id_{SO}\vec{l}\cdot\vec{s}W_{SO}h_{W_{SO}}(r) \quad (1)$$

where, $\vartheta_c$ (r) is the Coulomb term, $V(r), V_S(r), W_S(r), W_V(r), V_{SO}(r), W_{SO}(r)$ are energy-dependent well depths, $d_{SO} = (\hbar/m_\pi c)^2$ is the spin-orbit constant.

The real and imaginary volume terms $f_V$ and $f_W$ defined by Woods-Saxon shape as,

$$f_i = \frac{1}{1+exp[(r-R_i)/a_i]} \qquad i = V, W \qquad (2)$$

where $R_i$ and $a_i$ are the radii and the diffusivities, respectively.

Local and global parameter sets have been presented by various researchers for the deuteron optical model. The main ones are the studies of Watanabe’s (Watanabe, 1958), Daehnicket et al. (Daehnick et al., 1980), Bojowald et al. (Bojowald et al., 1988), Han et al. (Han et al., 2006) and Haixia et al. (An & Cai, 2006). Global deuteron potential of Daehnick et al. covers the target mass range of 27 ≤ A ≤ 238 and an energy range from 11.8 to 90 MeV. J. Bojowald et al. global potential covers the target mass range of 12 ≤ A ≤ 208 and the energy range from 52 to 85 MeV. Han et al. obtain deuteron global phenomenological optical model potential parameters for nuclides in the mass range 12 ≤ A ≤ 209 with incident energies from threshold up to 200 MeV. Haixia and Chonghai present set of global deuteron optical potential parameters, which it covers target nuclei ranging from $^{12}C$ to $^{238}U$ in the energy region below 183 MeV.

In the study, calculations were carried out using the TALYS (Koning et al., 2007) nuclear reaction code. TALYS is a nuclear reaction code that is widely used and gives very successful results for the reactions of light projectile particles (proton, neutron, deuteron, triton, alpha and $^3He$) and target nuclei larger than 12. There are five deuteron optical model potential (dOMP) options in TALYS 1.96/2.0 for the deuteron elastic and inelastic differential cross section calculations. The dOMPs selected in the study are the potentials included as options in the TALYS code. dOMPs, their refs. and Talys input parameter keywords were listed in Table 1. Detailed information about the mentioned deuteron optical potentials is available in the references.

**Table 1.** dOMPs, references and TALYS input parameter keywords of the models in the study.

| **The Deuteron Optical Model Potentials (dOMP)** | **Reference** | **Talys Keyword** |
|---|---|---|
| Watanabe folding approach | (Watanabe, 1958) | deuteronomp 1 |
| Deuteron potential of Daehnick et al. | (Daehnick et al., 1980) | deuteronomp 2 |
| Deuteron potential of Bojowald et al. | (Daehnick et al., 1980) | deuteronomp 3 |
| Deuteron potential of Han et al. | (Han et al., 2006) | deuteronomp 4 |
| Deuteron potential of Haixian An et al. | (An & Cai, 2006) | deuteronomp 5 |

Experimental elastic and inelastic differential cross section values for $^{14}N$ and $^{16}O$ target nuclei were taken from the study of Nguyen (Nguyen, 1966) and for $^{27}Al$ target nucleus from the study of Cowley et al. (Cowley et al., 1966) and the study of Jolly et al. (Jolly et al., 1963) via EXFOR Experimental Nuclear Reaction Data (Otuka et al., 2014). In this study, experimental data in the 14-15 MeV incident energy range was compiled in order to study within the framework of the compound nucleus reaction mechanism. Target nuclei in the study consist of light nuclei such as $^{14}N$, $^{16}O$ and $^{27}Al$.

## 3. Results and Discussion

Differential cross sections were calculated for elastic and inelastic scattering of 14-15 MeV energy range deuterons from $^{14}N$, $^{16}O$ and $^{27}Al$ targets. The calculations were carried out for the five different deuteron optical model parameter sets given as options in the TALYS nuclear code.

The elastic scattering differential cross-section graphs for $^{14}N$, $^{16}O$ and $^{27}Al$ target nuclei at 14. 25, 15 and 15.8 MeV incident energies are given in Figures 1-4.

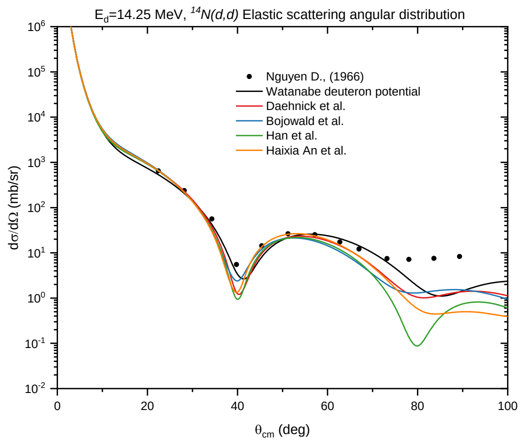


**Figure 1.** Calculated elastic scattering differential cross sections and experimental values for $^{14}N$ target nucleus at 14.25 MeV incident deuteron energy.

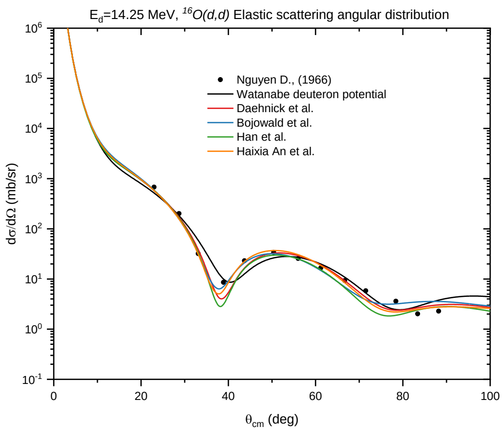


**Figure 2.** Calculated elastic scattering differential cross sections and experimental values for $^{16}O$ target nucleus at 14.25 MeV incident deuteron energy.

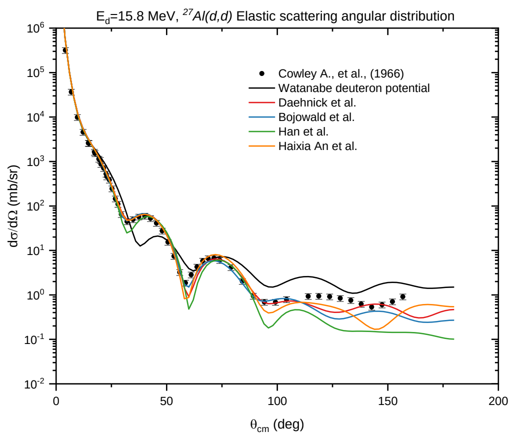


**Figure 3.** Calculated elastic scattering differential cross sections and experimental values for $^{27}Al$ target nucleus at 15.8 MeV incident deuteron energy.

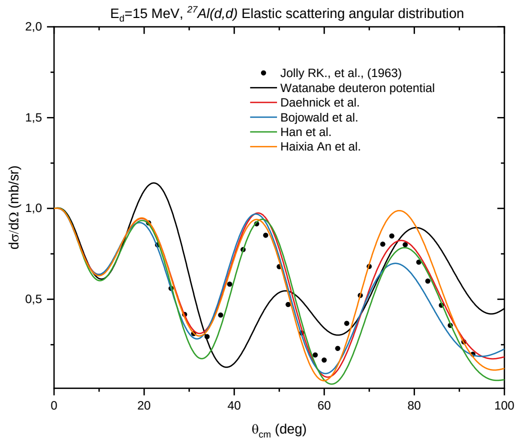


**Figure 4.** Calculated elastic scattering differential cross sections and experimental values for $^{27}Al$ target nucleus at 15 MeV incident deuteron energy.

In Figure 1 and Figure 2, although $^{14}N$ and $^{16}O$ have similar scattering angles, it is seen that there are deviations from the experimental values at large angles in the calculations performed for $^{14}N$. It is very likely that this deviation is due to experimental error. For the target nucleus $^{16}O$, angular distribution calculations are close to each other, and it can be said that the last two models are slightly more compatible with experimental data. In Figure 3, except for the potentials of Watanabe and Han et al., results close to each other and close to experimental values were obtained in the other three models. Similarly, in Figure 4, all calculations are compatible with the experimental points, except for Watanabe potentials.

The inelastic scattering differential cross-section graphs for $^{16}O$ and $^{27}Al$ target nuclei at 14. 25, 15 and 15.8 MeV incident energies are given in Figures 5-9.

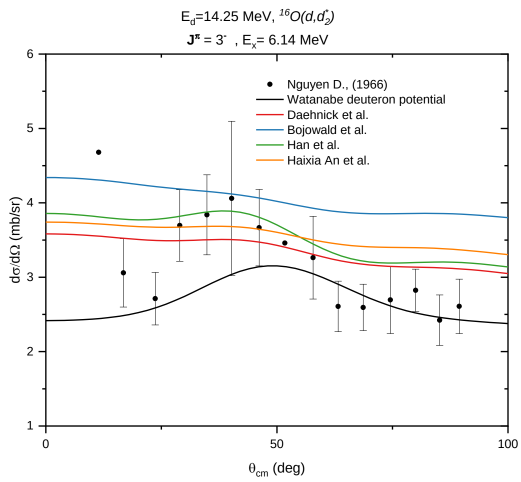


**Figure 5.** Calculated inelastic scattering differential cross sections and experimental values for $^{16}O$ target nucleus at 14.25 MeV incident deuteron energy.

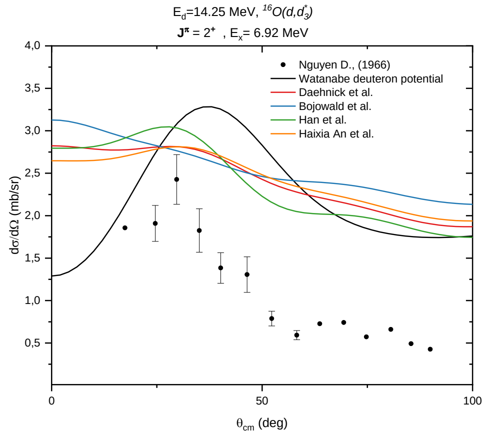


**Figure 6.** Calculated inelastic scattering differential cross sections and experimental values for $^{16}O$ target nucleus at 14.25 MeV incident deuteron energy.

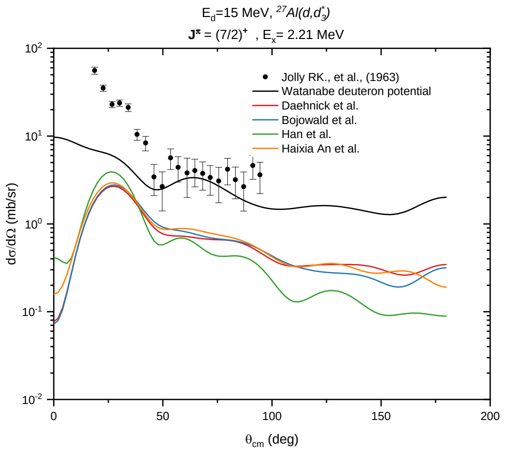


**Figure 7.** Calculated inelastic scattering differential cross sections and experimental values for $^{27}Al$ target nucleus at 15 MeV incident deuteron energy.

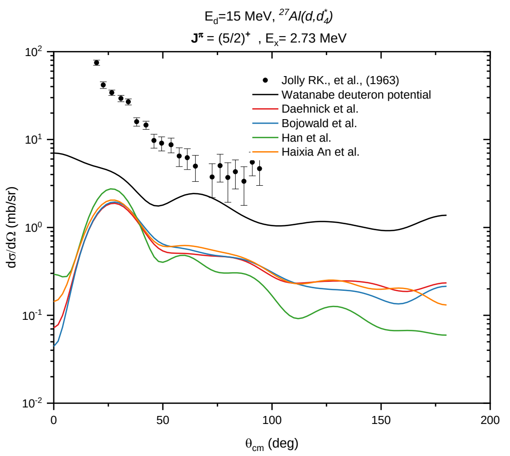


**Figure 8.** Calculated inelastic scattering differential cross sections and experimental values for $^{27}Al$ target nucleus at 15 MeV incident deuteron energy.

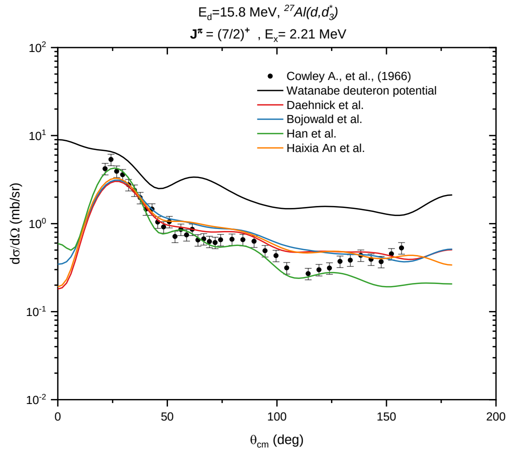


**Figure 9.** Calculated inelastic scattering differential cross sections and experimental values for $^{27}Al$ target nucleus at 15.8 MeV incident deuteron energy.

The inelastic scattering angular distribution for the second and third discrete state are shown in Figure 5 and Figure 6 for the $^{16}O$ target nucleus. While all of the models are compatible with the experimental data for the second discrete state angular distribution calculations, the success of the models is not sufficient for the third discrete calculations. Inelastic scattering angular distribution graphs of deuterons with incident energies of 15 MeV and 15.8 MeV for the $^{27}Al$ target nucleus are given in Figures 7-9. At 15 MeV incident energy, all potentials except Watanabe 's potential (in Figure 7 and Figure 8) could not agree with the experimental data at all scattering angles. Watanabe 's potential can be considered partially successful at the fourth discrete level calculations. At 15.8 incident energy, unlike Figure 7 and Figure 8, it was revealed that models other than Watanabe's potential were successful. In particular, the potential parameters prepared by Han et al. are in good agreement with the experimental values for this nucleus and incident energy.

In general, although the models achieved acceptable results in elastic scattering calculations, partially compatible results were obtained for inelastic scattering. It should also be noted that the calculations were made with the default settings of the Talys code. More successful results can be achieved by using other models and parameters included in the code.

## 4. Conclusion

In this study, elastic and inelastic differential cross sections of the scattering reactions of $^{14}N$, $^{16}O$ and $^{27}Al$ target nuclei and deuteron projectile particles at various energies were calculated using different global optical model parameters. The potentials of Han et al. and Haixian et al. were prepared in accordance with current experimental data. Therefore, it was expected to provide better agreement with experimental data. Their global potential parameters were partially successful in this study. Although the Watanabe potential is an older study, results were as successful as the results of the last two models. It was seen that the angular distribution calculations of inelastic scattering are far from the experimental data. This situation can be resolved by using other parameters included in the code.

Experimental data is an indispensable need to develop the nuclear optical model and obtain successful theoretical results. The success of scattering cross-section calculations for deuteron-inducted reactions is also possible with more experimental data. There appears to be a need for further experimental work in these types of reactions. With the increase in the number of experimental deuteron-introduced reaction studies, it will be possible to obtain more consistent optical model parameter sets in the future. It is also possible to study local optical model parameters for these nuclei in future studies.

## Conflict of Interest

The author has no conflict of interest to declare.

## References


An, H., & Cai, C. (2006). Global deuteron optical model potential for the energy range up to 183 MeV. *Physical Review C*, *73*(5), 054605. https://doi.org/10.1103/PhysRevC.73.054605

Bojowald, J., Machner, H., Nann, H., Oelert, W., Rogge, M., & Turek, P. (1988). Elastic deuteron scattering and optical model parameters at energies up to 100 MeV. *Physical Review C*, *38*(3), 1153-1163. https://doi.org/10.1103/PhysRevC.38.1153

Büyükuslu, H. (2017). Modelled excitation functions of 112,114,116,118,120,122,124Sn isotopes for an incident energy range of 10-80 MeV. *Celal Bayar University Journal of Science*, *13*(4), 925-928. https://doi.org/10.18466/cbayarfbe.370373

Cowley, A. A., Heymann, G., Keizer, R. L., & Scott, M. J. (1966). Elastic and inelastic scattering of 15.8 MeV deuterons. *Nuclear Physics*, *86*(2), 363-377. https://doi.org/10.1016/0029-5582(66)90544-X

Daehnick, W. W., Childs, J. D., & Vrcelj, Z. (1980). Global optical model potential for elastic deuteron scattering from 12 to 90 MeV. *Physical Review C*, *21*(6), 2253-2274. https://doi.org/10.1103/PhysRevC.21.2253

Han, Y., Shi, Y., & Shen, Q. (2006). Deuteron global optical model potential for energies up to 200 MeV. *Physical Review C*, *74*(4), 044615. https://doi.org/10.1103/PhysRevC.74.044615

Jolly, R. K., Lin, E. K., & Cohen, B. L. (1963). Angular distributions from elastic scattering of 15-MeV deuterons. *Physical Review*, *130*(6), 2391-2396. https://doi.org/10.1103/PhysRev.130.2391

Koning, A. J., Hilaire, S., & Duijvestijn, M. C. (2007). *TALYS-1.0.* International Conference on Nuclear Data for Science and Technology. Nice.

Nguyen, D. C. (1966). Elastic and inelastic scattering of deuterons from Be9, C12, N14 and O16 at 14 MeV. *Journal of the Physical Society of Japan*, *21*(12), 2462-2475. https://doi.org/10.1143/JPSJ.21.2462

Otuka, N., Dupont, E., Semkova, V., Pritychenko, B., Blokhin, A. I., Aikawa, M., Babykina, S., Bossant, M., Chen, G., Dunaeva, S., Forrest, R. A., Fukahori, T., Furutachi, N., Ganesan, S., Ge, Z., Gritzay, O. O., Herman, M., Hlavač, S., Kato, K., Lalremruata, B., & Zhuang, Y. (2014). Towards a more complete and accurate experimental nuclear reaction data library (EXFOR): International collaboration between nuclear reaction data centres (NRDC). *Nuclear Data Sheets*, *120*, 272-276. https://doi.org/10.1016/J.NDS.2014.07.065

Watanabe, S. (1958). High energy scattering of deuterons by complex nuclei. *Nuclear Physics*, *8*, 484-492. https://doi.org/10.1016/0029-5582(58)90180-9